A Wideband Dual Circular Polarization Horn Antenna for mmWave Wireless Communications

Chao Shu, Junbo Wang, Shaoqing Hu, Yuan Yao, *Senior Member, IEEE*, Junsheng Yu, *Senior Member, IEEE*, Yasir Alfadhl, *Member, IEEE*, Xiaodong Chen, *Fellow, IEEE*

Abstract—**This letter presents our design and experimental verification of a wideband dual circular polarized antenna operating in W-Band based on an optimised waveguide septum polarizer and a profiled smooth-wall horn. This antenna is capable of transmitting and receiving two orthogonal circular polarized signals (Left Hand Circular Polarization and Right Hand Circular Polarization) simultaneously to achieve Full-Duplex hence twofold spectrum efficiency for mmWave wireless communications. The fabricated antenna shows 21% relative bandwidth from 76.8 GHz to 94.7GHz with AR < 5.8 dB, the reflection coefficient is below -15 dB and isolation > 20 dB for both LHCP and RHCP.**

Index Terms—**millimetre wave, dual circular polarization, septum polarizer, profiled smooth-wall horn.**

I. INTRODUCTION

MILLIMETRE-WAVE (mmWave) wireless communications has attracted great interest in recent years and is considered as a promising technology that can provide high data rate for wireless links beyond 5G [1]. Over the past few years, much effort has been devoted to improving the transmission distance and the spectrum efficiency for mmWave wireless link [2][3]. A demonstration of 54-Gbps W-band signal transmission over a distance of 2.5 km is reported in [4], where two pairs of Cassegrain antennas with two orthogonal linear polarization are used to achieve both high gain and twofold data rate by applying Polarization Division Multiplexing (PDM), though there is a risk of polarization mismatch over such a long transmission distance.

Therefore, a dual circular polarized (CP) reflector antenna is preferred in mmWave communications. An attractive method to achieve dual circular polarization in microwave bands is based on the stepped septum polarizer that can also work as an Orthomode Transducer (OMT), leading to a compact size [5][6], especially for those dual CP feed horns [7]. A number of dual CP antennas are designed based on this septum polarize in circular waveguides in X-band [8] and K/Ka bands [9][10], but their relative bandwidths are around only 9% - 13%. In mmWave band, an antenna based on the septum polarizer at 225 GHz for radar system is proposed [11]. 30 dB isolation is

achieved within 10% of the bandwidth, but the aperture efficiency is only 34%. A dual CP antenna with 40% bandwidth operating in X-band based on septum polarizer with square waveguide is reported recently in [12] by employing a quad-ridged horn as the radiator. However, the isolation of its polarizer part is only 15 dB.

Therefore, we propose to design a dual CP antenna with wider bandwidth and better isolation for mmWave communications in W-band. This letter presents our design and experimental verification of a compact feed antenna with dual CP working in W-band based on a stepped septum polarizer, by applying a smooth-wall horn with an optimised profile and wideband waveguide transformer, wide bandwidth with good isolation and rotationally symmetric radiation pattern is achieved, which enables this antenna to offer full-duplex capability as well as the high gain when it is used together with only one reflector or Cassegrain reflector.

II. ANTENNA DESIGN

The structure of the complete antenna is shown in Fig. 1, consisting of three sections. The LHCP and RHCP signals generated by the stepped septum polarizer in a square waveguide will propagate through a square-to-circular waveguide transformer into a profiled smooth-wall horn. A pair of waveguide transformers with 90° E-plane bends are used to convert the input ports of the septum polarizer into standard WR10 rectangular waveguides. When port 1 is excited, LHCP will be generated; while port 2 is excited, RHCP will be generated.

A. Stepped Septum Polarizer

The geometry of the septum polarizer with a 4-step septum placing in the centre of a square waveguide is shown in Fig. 2. The dimensions of the square waveguide is designed so that only TE_{10} and TE_{01} mode can propagate through it within the working frequency range, which can be regarded as the vertical and horizontal components of circular polarization. With properly designed dimensions of steps, vertical and horizontal polarization components with same amplitude and ±90º phase shift can be excited to form a circular polarized electromagnetic field. The two rectangular ports of the polarizer are converted

Chao Shu, Shaoqing Hu, Yasir Alfadhl and Xiaodong Chen are with School of Electronic Engineering and Computer Science, Queen Mary University of London, London E1 4NS, UK (e-mail: xiaodong.chen@qmul.ac.uk).

Junbo Wang, Yuan Yao and Junsheng Yu are with School of Electronic Engineering, Beijing University of Posts and Telecommunications, Beijing, 100876, China.
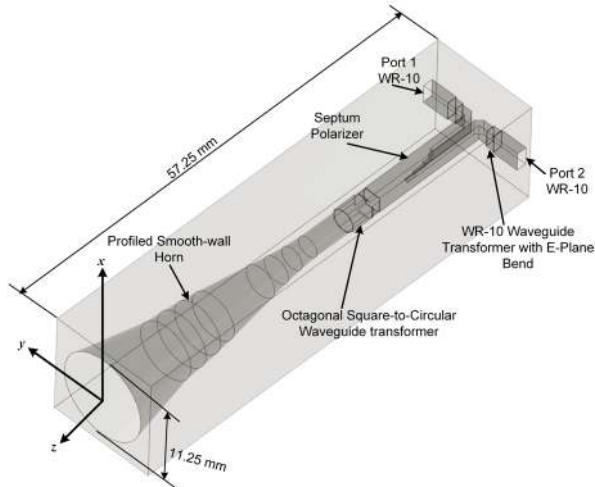
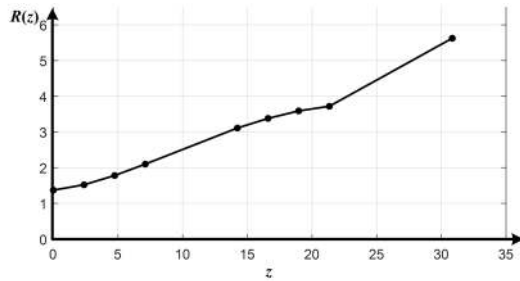Fig. 1. Structure of the complete antenna.

Fig. 2. Geometry of the septum polarizer.

Fig. 3. Profile of the smooth-wall horn.

Fig. 4. Photo of the fabricated antenna.

into two standard WR-10 rectangular waveguides (2.54 mm × 1.27 mm) by using a pair of 90° E-plane bends and transformers. The dimensions of the septum polarizer are optimised by using Nelder Mead Simplex and Particle Swarm Optimisation (PSO) Algorithm provided by CST MWS, and are listed in Fig 2.

B. Smooth-wall Circular Horn with Specific Profile

The whole profile of the smooth-wall horn is divided into two sections, as shown in Fig. 3. A sinusoid profile which is one of the empirical profiles [13] is selected for profile of the first section:

$$R(z) = sin^p(z) \qquad (1)$$

where R(z) is the radius and *z* is axial distance. The value of *p* is optimised to be 2.5 to achieve low reflection coefficient over wide bandwidth and rotationally symmetric radiation pattern. This section is discretized into seven linear segments for the ease of fabrication. A conical section is cascaded to add a degree of freedom in order to optimise further the overall performance of the antenna. The second section is optimised to follow a linear-tapered circular conical profile with radius changing from 3.72 mm to 5.625 mm in a length of 9.5mm.

C. Square-to-Circular Waveguide Transformer

A multi-section octagonal waveguide transformer [14] is applied to connect circular horn and the septum polarizer for ease of fabrication at the high frequency with wide bandwidth and a compact size. The reflection coefficient of this transformer is optimised to be lower than -30 dB across the entire bandwidth ranging from 75 GHz to 95 GHz.
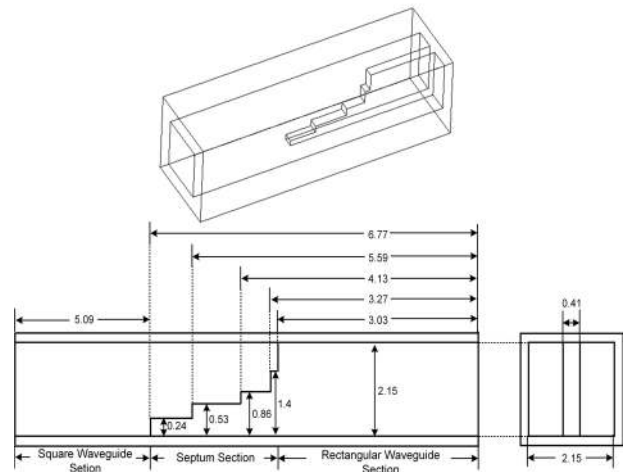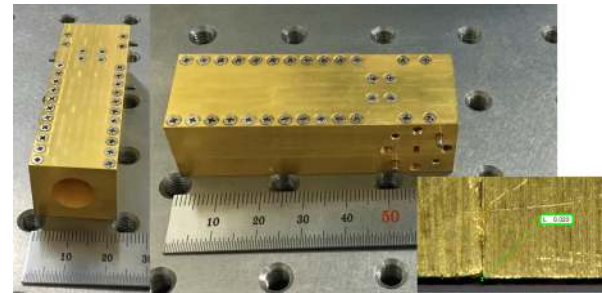
III. SIMULATION AND MEASUREMENT RESULTS

After the design of the complete antenna is optimised through simulation in CST MWS, a prototype of the proposed antenna is fabricated and measured by using a THz Vector Network Analyser (VNA) and an mmWave Compact Antenna Test Range (CATR). The fabricated antenna is shown in Fig. 4.

In the mmWave CATR, a linearly polarized horn in W-band connected to a motor is installed as a reference antenna which can be set to an arbitrary angle within 360° along its axis in order to measure the magnitudes of different polarization components of Antenna Under Test (AUT). The AUT and mmWave head was mounted on a re-adjustable supporting frame which is designed for this test to enable the radiation pattern and AR measurement in 0°(YZ)/45°/90°(XZ) planes while make sure the axis of AUT in the same position. The supporting frame was then mounted on a positioner where the AUT can be rotated horizontally to record the magnitudes with respect to azimuth (θ) for one polarization component.

The simulated and measured reflection coefficient as well as the isolation are illustrated in Fig. 5. As can be seen from the result, the measured reflection coefficient for both port 1 and port 2 are lower than -15 dB over the bandwidth from 75 GHz to 95 GHz, which agrees well with the simulated result. It can be observed that the measured isolation deteriorates at the edges of the band compared with the simulated result, due to the fabrication imperfection. But an isolation higher than 20 dB is still met within 76.8 – 94.7 GHz.

To measure the AR in a desired plane, the angle of reference antenna is set from 0° to 150° with a step of 30°, and for each angle, the AUT is scanned horizontally to record the
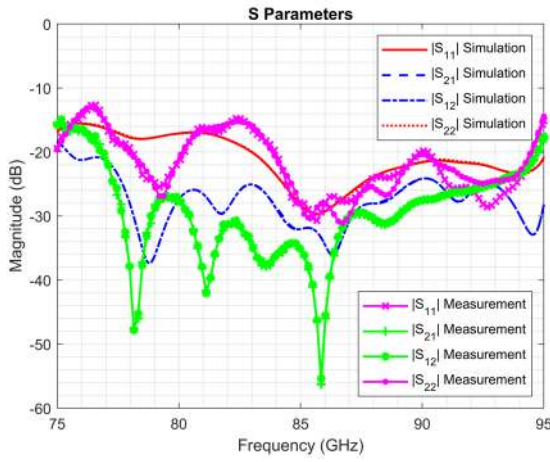
Fig. 5. Simulated and measured S parameters of the proposed antenna.

Fig. 6. Simulated and measured Axial Ratio of the proposed antenna.

magnitudes with respect to azimuth (θ) for this polarization components. After that, the polarization components with maximum and minimum magnitudes at θ=0° are considered as the major and minor axes of the polarization ellipse, and the ratio of the maximum to minimum magnitude defines the AR at the boresight of the AUT. By calculating the difference between these two selected curves, AR with respect to azimuth (θ) can be obtained.

Fig. 6 depicts the simulated and measured AR for both LHCP and RHCP at boresight, and the inset of Fig.6 shows an arc of the polarization ellipse measured in *yz* plane at 85 GHz as an example, whose polarization angle ranges from 0° to 150° with a step of 30°, and major and minor axes appear at 60° and 150° respectively. It can be found that the simulated AR is below 2dB. However, the measured AR ranges from 2.4 dB to 5.8 dB, much worse than the simulated results. The cause of this large discrepancy is mostly due to misalignment between the fabricated block halves. The fabricated antenna then has been investigated under a microscope and the approximate misalignment has been measured to be around 23 μm, which is shown in the inset of Fig. 4. To verify this, simulations were also conducted by introducing misalignments in the fabrication model deliberately. The dot lines in Fig. 6 depict the effect of misalignments of 20 and 24 μm on the AR, which agrees better with the measured results, and is consistent with the speculation and aforementioned measurement under a microscope.

According the obtained AR with respect to azimuth (θ), XPD with respect to azimuth (θ) can be derived, and together with total radiation derived from magnitudes of major and minor
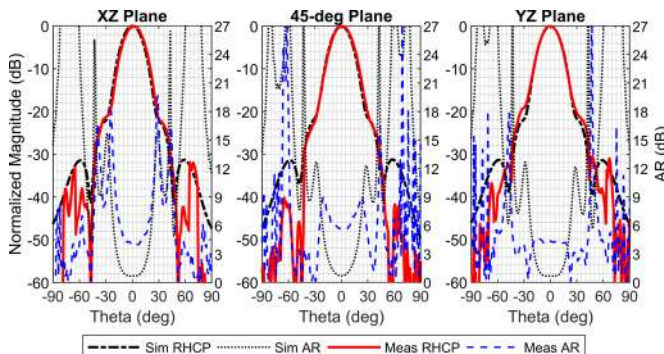
axes of the polarization ellipse, the LHCP/RHCP components can be calculated. The normalized radiation patterns in *xz*, *yz* and 45° plane at 85 GHz for LHCP and RHCP are shown in Fig. 7 and Fig. 8. It can be observed that there is a good agreement between the measured and simulated results. It can also be found that a good rotational symmetry is achieved, which makes it ideal as a primary feed for reflector antennas. The normalized radiation patterns for LHCP and RHCP in *xz*, *yz* plane and 45° plane at 75 and 95 GHz are presented in Fig. 9 - 12, which shows a good agreement between simulated and measured results as well as the stable radiation patterns across the band.

The antenna gain over the entire working bandwidth are shown in Fig. 11. The measured antenna gain is 18.3±2 dBic from 75 GHz to 95 GHz, which agrees with simulated one, the drop at 75 GHz and 95 GHz is probably due to the deterioration of S_{11} at the edges of the band which can be observed in Fig. 5.

IV. CONCLUSION

A wideband horn antenna with dual circular polarization is proposed and investigated in this letter. This antenna is designed based on a stepped septum polarizer and a profiled smooth-wall circular horn. A prototype is fabricated and measured, and the experimental results show that 21% relative bandwidth ranging from 76.8 GHz to 94.7 GHz is achieved with reflection coefficient S_{11} < -15 dB and isolation > 20 dB as well as AR < 5.8 dB for both LHCP and RHCP. The discrepancy between simulated and measured AR has been found to be mostly caused by the misalignment of the fabrication. In
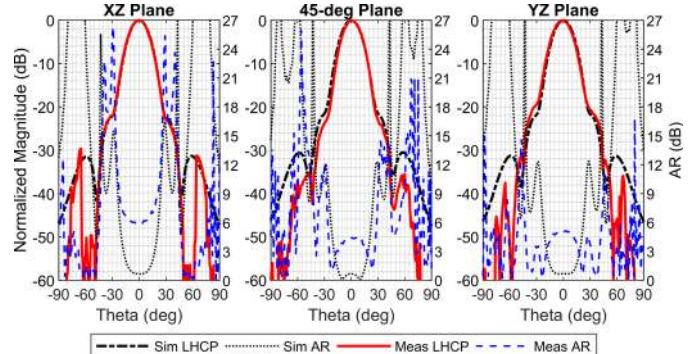

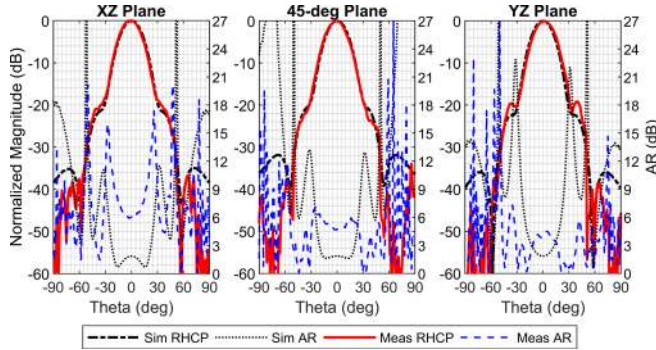Fig. 7. Simulated and measured radiation pattern for RHCP at 85 GHz.

Fig. 8. Simulated and measured radiation pattern for LHCP at 85 GHz.

> *This article has been accepted for publication in a future issue of this journal, but has not been fully edited. Content may change prior to final publication. Citation information: DOI10.1109/LAWP.2019.2927933, IEEE Antennas and Wireless Propagation Letters*
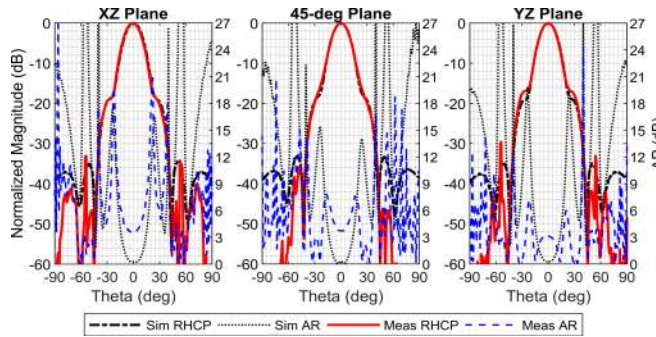
4

Fig. 9. Simulated and measured radiation pattern for RHCP at 75 GHz.

Fig. 10. Simulated and measured radiation pattern for LHCP at 75 GHz.
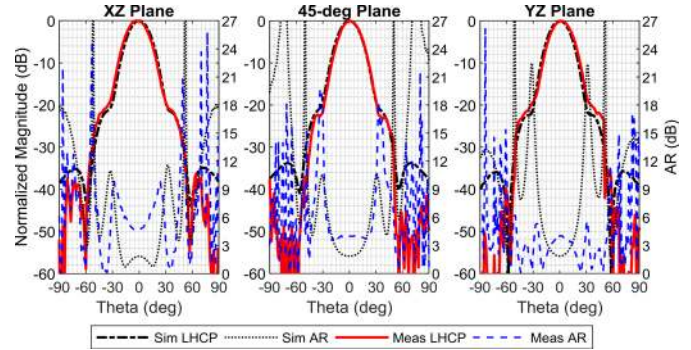

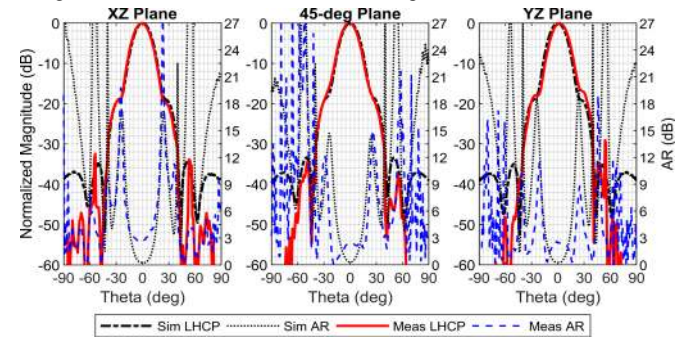Fig. 11. Simulated and measured radiation pattern for RHCP at 95 GHz.

Fig. 12. Simulated and measured radiation pattern for LHCP at 95 GHz.

addition, with rotationally symmetric and stable radiation pattern over the wide bandwidth, it is suitable to be used as a primary feed for reflector antennas, which can offer both high gain and Full-Duplex capability for mmWave communications.
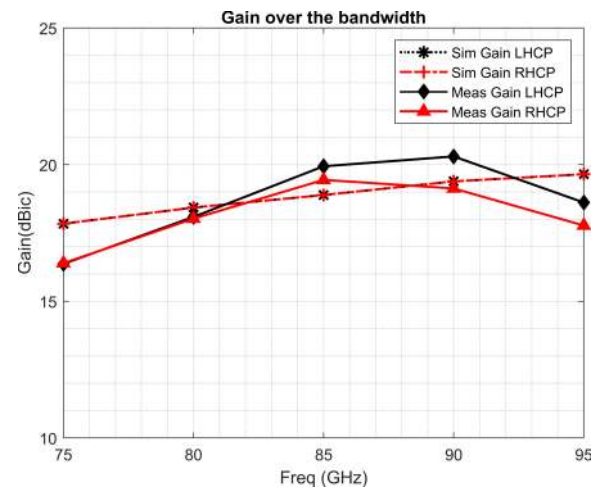
V. ACKNOWLEDGMENT

Fig. 13. Simulated and measured gains of the proposed antenna.

REFERENCES

[1] T. S. Rappaport, S. Sun, R. Mayzus, H. Zhao, Y. Azar, K. Wang, G. N. Wong, J. K. Schulz, M. Samimi, and F. Gutierrez, "Millimeter Wave Mobile Communications for 5G Cellular: It Will Work!," *IEEE Access*, vol. 1, pp. 335–349, 2013.

[2] A. Hirata, T. Kosugi, H. Takahashi, J. Takeuchi, H. Togo, M. Yaita, N. Kukutsu, K. Aihara, K. Murata, Y. Sato, T. Nagatsuma, and Y. Kado, "120-GHz-Band Wireless Link Technologies for Outdoor 10-Gbit/s Data Transmission," *IEEE Transactions on Microwave Theory and Techniques*, vol. 60, no. 3. pp. 881–895, 2012.

[3] X. Li, J. Yu, J. Zhang, Z. Dong, F. Li, and N. Chi, "A 400G optical wireless integration delivery system," *Opt. Express*, vol. 21, no. 16, pp. 18812–18819, 2013.

[4] X. Li, J. Yu, K. Wang, Y. Xu, L. Chen, L. Zhao, and W. Zhou, "Delivery of 54-Gb/s 8QAM W-Band Signal and 32-Gb/s 16QAM K - Band Signal Over 20-km SMF-28 and 2500-m Wireless Distance," *J. Light. Technol.*, vol. 36, no. 1, pp. 50–56, 2018.

[5] M. Chen and G. Tsandoulas, "A wide-band square-waveguide array polarizer," *IEEE Trans. Antennas Propag.*, vol. 21, no. 3, pp. 389–391, 1973.

[6] T. Ege and P. Mcandrew, "Analysis of stepped septum polarisers," *Electron. Lett.*, vol. 21, no. 24, pp. 1166–1168, 1985.

[7] R. Behe and P. Brachat, "Compact duplexer-polarizer with semicircular waveguide (antenna feed)," *IEEE Trans. Antennas Propag.*, vol. 39, no. 8, pp. 1222–1224, 1991.

[8] C. Kumar, V. V Srinivasan, V. K. Lakshmeesha, and S. Pal, "Novel Dual Circularly Polarized Radiating Element for Spherical Phased-Array Application," *IEEE Antennas Wirel. Propag. Lett.*, vol. 8, pp. 826–829,

2009.

[9] U. P. Hong, M. Schneider, and R. Gehring, "Slim Ka-band triple band polariser network for user and gateway antenna feed application," in *2017 47th European Microwave Conference (EuMC)*, 2017, pp. 1163–1166.

[10] G. Addamo, O. A. Peverini, D. Manfredi, F. Calignano, F. Paonessa, G. Virone, R. Tascone, and G. Dassano, "Additive Manufacturing of Ka-Band Dual-Polarization Waveguide Components," *IEEE Trans. Microw. Theory Tech.*, vol. 66, no. 8, pp. 3589–3596, 2018.

[11] C. A. Leal-Sevillano, K. B. Cooper, J. A. Ruiz-Cruz, J. R. Montejo-Garai, and J. M. Rebollar, "A 225 GHz Circular Polarization Waveguide Duplexer Based on a Septum Orthomode Transducer Polarizer," *IEEE Trans. Terahertz Sci. Technol.*, vol. 3, no. 5, pp. 574–583, 2013.

[12] G. Jazani and A. Pirhadi, "Design of dual-polarised (RHCP/LHCP) quad-ridged horn antenna with wideband septum polariser waveguide feed," *IET Microwaves, Antennas Propag.*, vol. 12, no. 9, pp. 1541–1545, 2018.

[13] C. Granet, "Profile options for feed horn design," in *2000 Asia-Pacific Microwave Conference. Proceedings (Cat. No.00TH8522)*, 2000, pp. 1448–1451.

[14] A. Mediavilla, J. L. Cano, and K. Cepero, "On the Octave Bandwidth Properties of Octagonal-Shaped Waveguide Mode Transformers," *IEEE Trans. Microw. Theory Tech.*, vol. 59, no. 10, pp. 2447–2451, 2011.